Hydrol. Earth Syst. Sci. Discuss., 9, 10011–10051, 2012
www.hydrol-earth-syst-sci-discuss.net/9/10011/2012/
doi:10.5194/hessd-9-10011-2012

Hydrology and Earth System Sciences Discussions

An effective depression filling algorithm for DEM-based 2-dimensional surface flow modelling

D. Zhu[1], Q. Ren[2], Y. Xuan[1], Y. Chen[3], and I. Cluckie[1]

[1]College of Engineering, Swansea University, Swansea, SA2 8PP, UK
[2]Technology Centre, Hydraulic and Hydropower Project, Guangdong Province, Guangzhou, 510635, China
[3]Joint Lab of Water Disaster and Hydroinformatics, Sun Yat-sen University, D402, Geography and Environment Building, Guangzhou, 510275, China

Received: 23 August 2012 – Accepted: 26 August 2012 – Published: 5 September 2012

Correspondence to: D. Zhu (d.zhu@swansea.ac.uk)

Published by Copernicus Publications on behalf of the European Geosciences Union.

Abstract

The surface runoff process in fluvial/pluvial flood modelling is often simulated employing a two-dimensional (2-D) diffusive wave approximation to described by grid based digital elevation models (DEMs). However, a serious problem of this approach may arise when using a 2-D surface flow model which exchanges flows through adjacent cells, or conventional rink removal algorithms which also allow flow to be exchanged along diagonal directions, due to the existence of artificial depression in DEMs. This study firstly analyses the two types of depressions in DEMs and reviews the current depression filling algorithms with a medium sized basin in South-East England, the Upper Medway Catchment (220 km^2) used to demonstrate the depression issue in 2-D surface runoff simulation by MIKE SHE with different DEM resolutions (50 m, 100 m and 200 m). An alternative depression-filling algorithm for 2-D overland flow modelling is developed and evaluated by comparing the simulated flows at the outlet of the catchment. This result suggests that the depression estimates at different grid resolution of DEM highly influences overland flow estimation and the new depression filling algorithm is shown to be effective in tackling this issue when comparing simulations in sink-dominated and sink-free digital elevation models, especially for depressions in relatively flat areas on digital land surface models.

1 Introduction

The Digital Elevation Model (DEM) is a digital representation of the ground surface topography or terrain which often is represented as a Cartesian grid, a triangulated irregular network (TIN) or as contour-based flow nets (Moretti and Orlandini, 2008). The regular DEM grid is convenient for calculation and conversion because of its relatively simple structure and can therefore be widely applied to topographic analysis and terrain visualisation. In terms of hydrological applications, DEM data can also be used for catchment delineation, river network definition and catchment characteristics extraction

HESSD

9, 10011–10051, 2012

(Gallant and Wilson, 2000). Many fully and semi-distributed hydrological model structures or parameterisations are based on the DEM, such as the overland flow module in MIKE SHE (Abbott et al., 1986; DHI, 2007), TOPMODEL (Beven, et al., 1995), SWAT (Arnold et al., 1993), GBDM (Yu, 1987) model and some other applications referred to Singh (1995). Since the DEM is an approximate approach to representing terrain characteristics, the accuracy of the topography and the related hydrological applications will depend on the quality of the DEMs, especially characteristics such as slope analysis, river network density, flow path and the topographic index.

The DEMs have to be made "hydrologically correct" before applied to the model. As most of DEMs contain numerous topographic depressions, which are defined as areas without an outlet and often referred to as sinks or pits (Zandbergen, 2006). In regular-grid DEMs, topographic depressions are recognised as an area having one or more contiguous cells that are lower than all of its surrounding cells. Unsurpringly these depressions often create difficulty in determining flow directions as the flow cannot continue downstream until the depressions are filled (Jenson and Domingue, 1988).

The removal of artificial depressions is therefore desired due to the widespeard use of high resolution DEMs produced by technologies like LiDAR and IfSAR (Zhu, 2009) as MacMillan et al. (2003) revealed that high resolution LiDAR-derived DEMs often contains a very large number of (mostly small) depressions because of greater surface roughness and finer resolutions. Most DEMs available today contain a substantial amount of depressions which represent the incorrect, spurious topographic errors (Martz and Garbrecht, 1998; Olivrea et al., 2000; Planchon and Darboux, 2001; Soille, 2004; Lindsay and Creed, 2005; Zandbergen, 2006). Locating and removing depressions in DEMs, therefore, remain as a necessary very first step of hydrological analysis.

Currently, most depression filling algorithms are based on the 1-D single flow direction, for instance, Rho4/Rho8 (Fairfield and Leymarie, 1991), D8 (O'Callaghan and Mark, 1984), the Lea (1992) algorithm, D∞ (Tarboton, 1997). The algorithm developed by Jenson and Domingue (1988) is most widely used and has been implemented in many GIS and hydrological softwares, such as ArcMap (ESRI 2010), GRASS (GRASS

HESSD
9, 10011–10051, 2012

Development Team, 2003), HEC GEO-HMS (USACE, 2002), TOPOZ (Garbrecht and Martz, 1997), Arc Hydro Tools (Maidment, 2002), etc., all of which have been proved to be quite effective in one-dimensional surface runoff models. Nevertheless, the conventional depression filling algorithms are computationally intensive and very time-consuming, in particular processing high resolution DEMs. In order to improve the efficiency of identifying and filling surface depressions in DEMs, Wang and Liu (2006) proposed a depression filling method which can simultaneously determine flow paths and spatial partition of watersheds with one pass of processing, assisted by a novel concept of spill elevation and the least-cost search for optimal flow paths. And the time complexity of this method is in $O(N \log N)$, which is superior to any other depression filling algorithms (Wang and Liu, 2006).

However, accurate flow prediction over complex topography is required by fluvial/pluvial flood models which often adopt a one-dimensional (1-D) representation of channel flow linked with a 2-D description of flow over the floodplain, for example, TELEMAC-2D (Galland et al., 1991), FLO-2D (O'Brien, et al., 1993), LISFLOOD-FP (Bates and De Roo, 2000), AOFD (Maksimović et al., 2009). All these 2-D surface flow modelling usually involve a diffusion-wave treatment, which is commonly based upon determining the magnitude of flow between any two adjacent cells according to the water surface elevation difference and the Manning equation (Lane, 1998; Wheater, 2002; Yu and Lane, 2005). The differences between the 1-D and 2-D dynamic runoff processes lie in the fact that the 2-D surface flow model implies drainage along four possible directions (D4), not only receiving flow from upstream in x, y directions, but also draining to the downstream in x, y directions. Whereas the traditional 1-D overland flow path is determined by considering eight possible directions (D8), only receiving and draining the water in one direction. As a consequence, some non-depression DEM cells within D8's concept may unfortunately become depressions during the 2-D surface flow process, due to the inconsistency between D4 drainage used in 2-D surface runoff models and sink removal algorithms designed to work in combination with D8 flow direction algorithms.

HESSD
9, 10011–10051, 2012

For example, the elevation in x, y directions control the flow path, as illustrated in Fig. 1, and the arrows represent the flow direction on the surface. The depression cells as those shaded in Fig. 1a have lower elevations than the surrounding cells. The water in these depressions does not start to flow until the water level reaches 381 m and 386 m, respectively, and in this study these depressions are categorized as Type A. By comparisons, the elevations of the shaded cells in Fig. 1b are lower than the cells draining along cardinal flow directions but higher than the cells draining along diagonal flow directions, which are recognised as Type B depression. It is clear that for Type B (as in Fig. 1b), the cells with elevations 385 m, 364 m and 295 m starts to flow when the water level is increased to 406 m, 386 m and 340 m, respectively.

The Type A depression presented in Fig. 1a is quite common and can be conveniently removed by applying any existing depression filling algorithms mentioned above. However, the Type B depression formed by the DEM presented in Fig. 1b has two different scenarios. The two algorithms D8 and D4 for determining the overland flow path, are depicted by Fig. 2a, b, respectively. In this instance, all the water drained to the DEM boundary and the D8 algorithm as shown in Fig. 2a produced no “sinks”. By comparison, there is a sink in Fig. 2b due to the fact that the algorithm (D4) does not take into account the diagonal flow paths. Therefore, the water in the grid with a 295 m elevation will not flow until the water level increases to 340 m.

Therefore, the Type B depression can still be removed by applying filling algorithms based on the D8 assumption. But, it is less likely to be identified and removed in 2-D surface flow modellings, which employ D4 algorithm. And as consequences, it has greater impacts on the surface flow using 2-D described computations, in terms of affecting the kinematic wave celerity directly and hydraulic diffusivity indirectly (Orlandini and Rosso, 1998). However, there is a dearth of comprehensive studies examining the effects of depression removal on the 2-D surface flow modelling.

One possible approach as suggested by Zhu (2009), is to extend the river network to those Type B sinks by adding some arbitrary tributaries able to drain the ponded water back to the river. This method was shown to be very efficient in terms of getting back

HESSD
9, 10011–10051, 2012

from the sinks. However, adding tributary manually means it impractical to apply this approach to the case in which many ponds scatter across the catchment. Furthermore, subjectivity and uncertainty are inevitably brought in as to determining the paths and locations of these tributaries.

Wang and Liu (2006) proposed an effective 1-D depression filling algorithms for high resolution DEMs. This method can simultaneously determine flow paths and spatial partition of watersheds with one pass of processing by employing the innovative concepts of spill elevation and using least-cost search for optimal flow paths. It has been proved that their method outperforms the conventional filling algorithm in terms of the running time and effectiveness. However, similar to other 1-D depression filling approaches, it cannot be adapted in the DEM sink-remove process for 2-D overland flow modelling. Therefore, we propose a new method aiming to effectively fill the Type B depression for 2-D overland flow modelling in this paper, based on the fundamental computational concept of Wang and Liu (2006)'s 1-D filling algorithms, but has been modified and extended for the DEM requirements of 2-D surface flow modelling. Further, a rural catchment, Upper Medway Catchment (220 km^2 in south east of England) is taken as a case study on the impacts of the filling algorithms to overland flow modelling and whole catchment outflow modelling. As the representative of 2-D surface model, the MIKE SHE model (DHI, 2007), in particular its overland flow module, is chosen to analyse and assess the performance of the new depression filling algorithm.

2 The 2-D overland flow calculation

As a representative of a set of 2-D mathematical surface models, the MIKE SHE model has been widely used across the world and is capable of adapting DEM with various resolutions. In this study, the MIKE SHE model is to demonstrate the issues associated with artificial depression and to study the effectiveness of the new depression filling algorithms for 2-D surface modeling. It is expected that the result would be conveniently

HESSD
9, 10011–10051, 2012

applicable to a number of other modeling systems that share the similar 2-D surface flow approach as in MIKE SHE.

The overland flow module in MIKE SHE employs a simplified set of Saint Venant equations: the diffusive wave approximation describing the water movement on the surface and the finite difference method are used to solve this equation (DHI, 2007).

The Saint Venant equations are also called the one-dimensional unsteady open channel flow shallow water equations. If the Cartesian (x, y) coordinates are applied in the horizontal plane, the flow depth on the ground surface can be denoted by $h(x, y)$ and the flow velocity in the x- and y-directions is $u(x, y)$ and $v(x, y)$, respectively. Therefore, according to the conservation of mass, the net rainfall $i(x, y)$ added to the overland flow would be established as:

$$i = \frac{\partial h}{\partial t} + \frac{\partial}{\partial x}(uh) + \frac{\partial y}{\partial x}(vh) \tag{1}$$

where the momentum equations are:

$$\begin{cases} S_{\mathrm{fx}} = S_{\mathrm{Ox}} - \frac{\partial h}{\partial x} - \frac{u}{g}\frac{\partial u}{\partial x} - \frac{1}{g}\frac{\partial u}{\partial t} - \frac{qu}{gh} \\ S_{\mathrm{fy}} = S_{\mathrm{Oy}} - \frac{\partial h}{\partial y} - \frac{v}{g}\frac{\partial v}{\partial y} - \frac{1}{g}\frac{\partial v}{\partial t} - \frac{qv}{gh} \end{cases} \tag{2}$$

and the S_{f} and S_{O} stand for the friction slopes and ground surface slope respectively in x- and y-directions,

It is still numerically challenging to solve the two-dimensional Saint Venant equations dynamically. Thus the diffusive wave approximation method is introduced in MIKE SHE, which neglects the momentum losses (last three terms of the momentum equations) due to the local and convective acceleration and lateral inflows perpendicular to the flow direction. So the diffusive wave approximation in x- and y-directions is described below, given the relationship that $Z = Z_{\mathrm{g}} + h$, where Z_{g} is ground surface level. Hence,

$$\begin{cases} S_{\mathrm{fx}} = -\frac{\partial Z_{\mathrm{g}}}{\partial x} - \frac{\partial h}{\partial x} = \frac{\partial z}{\partial x} \\ S_{\mathrm{fx}} = -\frac{\partial Z_{\mathrm{g}}}{\partial y} - \frac{\partial h}{\partial y} = \frac{\partial z}{\partial y} \end{cases} \tag{3}$$

HESSD
9, 10011–10051, 2012

However, when the slope of the water surface profile is very shallow and the water movement is very slow, numerical problems will occur between the neighboring cells and any backwater simulations. Hence, the Strickler/Manning's coefficient K is employed for each friction slope and the diffusive wave approximation equations then become:

$$\begin{cases} \frac{\partial z}{\partial x} = \frac{u^2}{K_x^2 h^{4/3}} \\ \frac{\partial z}{\partial y} = \frac{v^2}{K_y^2 h^{4/3}} \end{cases} \tag{4}$$

Here the uh and vh represent discharge per unit length along the cell boundary and can be written as:

$$\begin{cases} uh = K_x(-\frac{\partial z}{\partial x})^{1/2} h^{5/3} \\ vh = K_y(-\frac{\partial z}{\partial y})^{1/2} h^{5/3} \end{cases} \tag{5}$$

The Manning M, ranging from 10 $m^{1/3}\,s^{-1}$ (rough channels) to 100 $m^{1/3}\,s^{-1}$ (smooth channels), is used in MIKE SHE to control the flow velocity. It is equivalent to the Strickler roughness coefficient, which is also defined as the inverse of the Manning's number.

MIKE SHE overland flow module employs finite difference technique to solve the Saint Venant equations. If the overland flow on the grid is considered as shown in Fig. 3, at time t having the length Δx and Δy and water depth of $h(t)$.

Then, the velocity terms of the finite difference form of Eq. (1) can be derived from the approximations as below:

$$\begin{cases} \frac{\partial(uh)}{\partial x} \cong \frac{1}{\Delta x}\{(uh)_E - (uh)_W\} \\ \frac{\partial(vh)}{\partial y} \cong \frac{1}{\Delta y}\{(uh)_N - (uh)_S\} \end{cases} \tag{6}$$

Where the quantity of flow in each direction are denoted by the subscripts, for instance, the $\Delta x(uh)_E$ is the volume flow across the eastern boundary. Therefore, the total water

HESSD
9, 10011–10051, 2012

that flows into the square across its north, south, east and west boundaries is described as and $\sum Q = Q_N + Q_S + Q_E + Q_W$ and Δh could be defined by Eq. (7):

$$\Delta h = h(t + \Delta t) - h(t) = i\Delta x^2 + \frac{\sum Q \Delta t}{\Delta x^2} \tag{7}$$

where i is the net input to overland flow from Eq. (1).

If the flow across the boundary between the squares (see Fig. 4), then Z_U and Z_{UD} stand for the higher and lower water levels, respectively, and the water depths in the square corresponding to Z_U and Z_D are h_U and h_D. Then, the discharge between the grids can be calculated by Eq. (7) combined with the Eq. (5). Hence,

$$Q = \frac{K\Delta x}{\Delta x^{1/2}} (Z_U - Z_D)^{1/2} h_u^{5/3} \tag{8}$$

Where the K is the Strickler coefficient and the water depth h_U is the free water that flows into the next grid, which is equal to the actual water depth minus the detention storage, since the detention storage is the ponded water that is trapped in the shallow surface depression. The overland flow into the cell could be zero if the upstream depth is zero or the water level in the cells is the same.

3 Depression filling algorithm

In order to tackle the depression issues that may exist in the 2-D surface modelling, a depression filling algorithm was developed based on Wang and Liu's (2006) methodology, consisting of two fundamental concepts: spill elevation and optimal spill path. Spill elevation is defined as the minimum elevation that the flow level in one cell needs to be raised in order to reach the catchment boundary and the path it takes was referred to as the optimal spill path. Therefore, the elevation of a grid cell does not need to be raised if it is high enough to establish a downslope flow path to an outlet at the edge of the DEM, and its spill elevation is the same as its original elevation value of the cell of DEM. Otherwise, we need to raise that cell from its original elevation to its spill elevation.

As water flows with the gravity force from a place with a high elevation to a place with a lower elevation. A downslope flow path consists of a series of connected cells to an outlet of the DEM has to be found and constructed without the depressions. In that case, the elevations of all the cells on the flow path are ensured to be non-decreasing from the outlet on the boundary to the interior cells, as the search of flow paths are always started from outlets.

As described in the previous section, the overland flow calculation process in the MIKE SHE model has multiple flow directions. Each non-depression cell not only receives flow from upstream in x, y directions, but also drains to the downstream in x, y directions. Therefore, the depression filling algorithm can comprise of four different single flow direction processes. If the flow in one particular cell can reach the catchment outlet without depression filling, then the elevation of all the cells on the path are in non-rising order, and vice versa. Hence, if there is no such pathway to connect the cells and the catchment outlet, the depression cells need to be raised sequentially to their spill elevation values to satisfy the condition that the elevation is non-decreasing. The spill elevation is used as the "cost" to search the optimal spill paths within the catchment, also known as the "least-cost search" algorithm.

This algorithm is represented in the C++ program by employing the concept of the "priority queue" method, in which the top priority elements are listed in the front. When it is applied to the 'least-cost search' algorithm, the top priority element is the least-cost path and the order of the queue follows the same rule.

Three member functions are involved in this method, PQueue.Push(), PQueue.Pop() and PQueue.Top(), which are used respectively to insert the element into the queue, delete the first element in the queue and then return to the first element of the queue. Table 1 shows the pseudo-code for this method: lines 1–5 initialise the priority queue, in which all DEM cells on the catchment boundary or river networks are regarded as

HESSD
9, 10011–10051, 2012

potential watershed outlets. In line 2, the spill elevation values of the outflow cells are allocated by their corresponding original elevation values. In line 3, the boundary cells are inserted into the priority queue through the member function PQueue.push(). In line 4, the processed outflow cells are marked. The while loop in lines 7–19 accomplish the search and expansion of the trees of optimal paths. Line 8 obtains the node with the least cost (the lowest spill elevation) through the member function PQueue.Top() and this least-cost node is deleted from the queue through the member function PQueue.Pop() in line 9. This series of procedures is labelled in the matrix Mark in line 10 to show that the least-cost node was process. The for loop in lines 11–18 starts to search the optimal paths from the four neighbourhood cells of the least-cost node. If any one of those four cells has not yet been processed before, the spill elevation value of the cell will be denoted by the higher value between the spill elevation value of the least-cost node and its original elevation value. In line 16, all of the other non-processed cells are inserted into the priority queue through the member function PQueue.push(). Then, the computation enters the second round until the priority queue is empty, so that all the DEM cells are processed in the end.

Additionally, Fig. 5a illustrates the DEM after this depression removal algorithm applied, using the same DEM example showed in Fig. 2. The order of algorithm processing the DEM is indicated in Fig. 5b. It shows that the algorithm took the cells on the boundary as the priority and listed all the surrounding cells into the process tree, then the cell with value 340 was considered as the search centre due to the least cost principle and the algorithm iterated until all the possible flow paths were searched and all the cells were processed.

4 Case study

Regarding the performance of this algorithm introduced above, the rainfall-runoff simulation of the Upper Medway Catchment (located South of London in the UK) was selected as a case study, assessing the suitability and effectiveness of the algorithm

Discussion Paper | Discussion Paper | Discussion Paper | Discussion Paper |

HESSD
9, 10011–10051, 2012
DEM-based 2-dimensional surface flow modelling
D. Zhu et al.

applied to the MIKE SHE 2-D surface hydrological model. In this study, various DEM with different resolutions were input into the MIKE SHE overland module and comparisons made between the raw DEM data, and the DEM data with the filling algorithm processing invoked, in terms of the volume of overall overland flow and the whole catchment outflow draining to the outlet.

In order to analyse the scale effect, three DEM datasets with different resolutions were resampled from the original 10 m resolution DEM data derived from the Ordnance Survey Land-Form Profile DTM (1 : 10 000) provided by EDINA Digimap service. The bilinear interpolation was employed to alter and produce a coarser resolution of the raster data, since it is preferred for data where the location from a known point or phenomenon determines the value assigned to the cell (that is, continuous surfaces), such as elevation and slope are all phenomena represented as continuous surfaces and are most appropriately resampled using bilinear interpolation. This interpolation algorithm uses the value of the four nearest input cell centres to determine the value on the output raster. The processing cells was identified by the nearest cell centre on the input raster and assigned itself to that value. This process is repeated for each cell in the output raster. The new value for the output cell is a weighted average of these four values, adjusted to account for their distance from the centre of the output cell. This interpolation method results in a smoother looking surface than can be obtained using the nearest neighbour. This numerical process is effectively a "low-pass" filter operation and to some extent introduces smoothing to the data field that helps remove high-frequency noise generated by the interpolation algorithm.

The Upper Medway catchment topography varies between around 30 m and 240 m above mean sea level. The majority of the slope characteristic in the Upper Medway Catchment varies from 2° to 8°, which represents about 70 % of the whole catchment and suggests that the landscape of the Upper Medway Catchment is made up of small hills surrounding the flat, low-lying relief of the floodplain without much variation of elevation (see Fig. 6).

HESSD
9, 10011–10051, 2012

As the catchment area is around 220 km^2, it is not feasible to use the 10 m resolution DEM as a topographic input in terms of the computational cost and the model calculation capability. Therefore, the 10 m resolution DEM was resampled to a coarser raster for three different resolutions (50 m, 100 m and 200 m) and the depression-filling algorithm then processed these up-scaled DEMs. All these DEMs (original and the ones after sink removal) were then analysed in ArcGIS before being put into the model.

Figure 7 shows the analysis of the cumulative distributions of DEM slopes as a fraction of the catchment area, which not only clearly indicates the considerable smoothing effect that has taken place as a consequence of resampling the elevation data (from 10 m to coarser resolutions) but also suggests that the depression filling algorithm using three different scales has not altered the general characteristics of the catchment in terms of the topographic properties.

Similarly Table 2 shows the comparison of slopes of the DEM at three different resolutions – before and after the depression filling algorithm was applied – in terms of the statistics of the slope in degrees. This did not reveal a clear difference between the DEMs before and after the sink removal but indicated that the general slope of the catchment decreased during the DEM resampling as a result of the averaging process being applied.

However, the comparisons in Table 2 in terms of elevation show little difference between the DEMs before and after the sink removal, as well as in the resampling impact because the statistics of elevation can only reflect the general characteristics of terrain, rather than indicating the changes that may impact processes on each DEM cell.

Figures 8–10 also illustrate the elevation differences after the depression filling algorithm was applied to different DEM resolutions: this is the terrain elevation after the filling algorithm process minus the original elevation value. The three figures suggest that most of the elevation values in the catchment remained quite similar after the depression filling algorithm had been applied, and most of the elevation differences occurred near the existing river network, implying that the depression filling algorithm

HESSD
9, 10011–10051, 2012

DEM-based 2-dimensional surface flow modelling

D. Zhu et al.

had made an effort to form synthetic river paths in order to drain the surface water to the river network.

More importantly, the statistics of depressions on the catchment shows that number of depressions in 50 m, 100 m and 200 m resolution DEMs detected by this filling algorithm were 3407, 1778 and 768, respectively, which made the corresponding area covered by the depressions were 8.52 km^2, 17.78 km^2 and 30.72 km^2 and the related proportion of whole catchment area were 3.87 %, 8.08 % and 13.96 %. It implied that resempling the DEMs to coarser resolution decreased the number of pits but the total area covered by sinks increased, which is consistant with the conclusion drawn by Grimaldi et al. (2007). Additionally, Table 3 indicates that the coarser DEM resolution produced more elevation differences after the filling algorithm process that will result in more differences in the volume of depression water on the surface, which matches the depression analysis in the previous section.

In order to test the impact of the depression algorithm on the surface flow, firstly, only the overland flow module was included in the MIKE SHE model, without any other input from the infiltration and groundwater interaction modules. Therefore the whole rainfall-runoff model was driven entirely by the terrain elevation and the Manning's number. All the DEMs were compared in the context of the MIKE SHE hydrological modelling structures in terms of the simulation flow at the catchment outlet (see the location in Fig. 3). The corresponding overland flow simulations are shown in Figs. 11–13.

Figure 14 shows the accumulated water depth on the surface during the model simulation. Given the same amount of precipitation, the accumulated surface water depth derived from the three original DEM inputs indicated that the proportions of surface detained water after the flow simulation were 17.68 %, 36.03 % and 55.84 %, respectively, suggesting that the resampled coarser raster resulted in more detained water on the catchment surface than the fine resolution DEM. In addition, more than half of the precipitation was retained on the surface when using the 200 m resolution DEM simulation, meaning that far less water drained to the river network when compared to the 50 m resolution results.

However, after the depression-filling algorithm was applied, the processed DEM produced similar detained accumulated surface water in the model, the corresponding proportions decreasing to 14.12 %, 17.80 % and 12.62 %. This indicated that the depression filling algorithm had efficiently eliminated ponds affecting the overland flow in MIKE SHE and the margins between the different DEM resolution simulated flows through the model were significantly reduced.

Figure 14 also shows that the algorithm-processed DEM with 100 m resolution produced similar accumulated surface water depth with the 50 m resolution raw DEM in the MIKE SHE model, implying that these two sets of DEM data can generate a similar amount of overland flow in the model. In this case, owing to the similarity of the accumulated surface water depth, all the DEMs with different resolutions after sink removal by the algorithm produced a similar amount of water on the surface. Thus the depression filling algorithm proposed in this study demonstrated a consistent performance in the MIKE SHE overland flow module, regardless of the resolution of the DEM data.

Secondly, the whole catchment rainfall-runoff simulation including subsaturated zone and saturated zone components in the MIKE SHE was carried out for further investigation of the efficiency of algorithm applied in this study. The water movement through the soil profile, along with the evapotranspiration is modelled by a simplified two-layer ET/UZ model, which is suited to be applied to the catchment that has a shallow groundwater table and used in the unsaturated zone to calculate the actual evapotranspiration and the amount of water that recharges the saturated zone. The ground water flow is calculated using the linear reservoir method and this method can be regarded as the balance of the data availability of the geology, the complexity of the groundwater simulation and the benefit from the model simplicity. The whole model was set up using a grid size of 100 m × 100 m. The trial-and-error parameterisation was employed and Nash-Sutcliffe efficiency (Nash and Sutcliffe, 1970) in calibration and validation was 0.93 and 0.91 (Zhu and Cluckie, 2012; Zhu, 2009).

Figures 15 to 17 shows the difference on the peak flow simulation at catchment outlet before and after the depression-filling algorithm was applied. The result of using

HESSD
9, 10011–10051, 2012

three DEM resolutions imply that the increase of overland flow due to the depression filling algorithm has significant impact on the total outflow, especially using the coarse DEM resolution in the model. Compared to the measured peak flow, Table 4 indicates that difference between modelled peak flow and observed peak flow on all DEM resolutions in this study were reduced, after the depression filling algorithm was employed. Additionally, similar to the previous overland flow simulation results, the coarser DEM resolution, the more impact on the peak flow caused by the depression filling algorithm. Therefore, the 200 m DEM resolution with depression-filling algorithm applied generates the best peak flow (closest to the measurement) throughout the study. Additionally, the increase of total outflow caused by the depression filling algorithm, shown in Table 4, all has been contributed to the peak flows during the simulations, which were clearly displayed in Figs. 16 and 17, for 100 m and 200 m DEM resolution, respectively. It suggests that the improvement of the model simulations benefit from the overland flow component after the depression filling algorithm is employed.

5 Conclusions

In this study, two different types of depressions in DEM data were discussed in the context of distributed hydrological modelling. It shows that the Type B depression is unlikely eliminated by the traditional 1-D depression filling algorithm when employing a 2-D surface flow model, which describes gravity-driven flows across terrains by employing 2-D diffusive wave approximation to propagate the surface water into the river channel. A close investigation shows that the problems in fact arise from the inconsistency between D4 drainage used in 2-D surface runoff models and the sink removal algorithms designed to work in combination with D8 flow direction algorithms.

A new depression-filling method was then developed following Wang and Liu's algorithm, in order to tackle the issue in 2-D flow flows. The MIKE SHE model was selected in this study to serve as an example of 2-D surface runoff modeling using the new depression-filling method. The comparisons between the MIKE SHE simulation with

HESSD
9, 10011–10051, 2012

original DEM and that applying the depression-filling method clearly indicated that the algorithm could efficiently eliminate the impact of artificial depression storage in DEM that could affect the surface flow calculation of the 2-D overland flow module in MIKE SHE.

The effect of DEM resampling was also investigated in this study using the 10 m DEM as a start and then gradually up-scaling it to 50 m, 100 m and 200 m resolution, respectively. The flow simulations using these DEMs with different resolution suggests that the DEM up-scaling process may result in more depressions and consiquently a higher degree of precipitation being accumulated on the catchment surface rather than being drained into the river network.

In terms of modelling overall catchment response it is important to note that once water from precipitation is in the channel network then it enters a much faster flow domain where the dynamic nature of flood response is generally determined. Conversely, water retained in artificial sinks across a DEM domain will be subject to a much slower catchment response. The outflow simulations of whole catchment by MIKE SHE indicate that the increased overland flow due to the application of the depression-filling procedure has considerable impact on the peak flow in particular and therefore improve the performance of the hydrological model. Again it implies that the depression filling algorithm is efficient and suitable for adoption in the 2-D surface flow models, not only because it produces more accurate surface flow but because it also reduces the uncertainties introduced by the spatial resampling of the DEM data. Furthermore, it has been shown that the overland flow simulations with coarser DEM can benefit more from using the depression-filling method as the artificial depressions are more likely to appear and have more impacts on the accuracy of simulations. This suggests that this depression-filling algorithm has a considerable potential for improving 2-D hydrological simulation over areas with insufficiently high resolution of DEM.

It is worth noting that the aim of this study was to examine the impact of depression removal on surface flows modelling using DEM and two-dimensional diffusive code in particular. And it was not meant to improve the description of surface runoff dynamics

HESSD
9, 10011–10051, 2012

Title Page
Abstract | Introduction
Conclusions | References
Tables | Figures
◂◂ | ▸▸
◂ | ▸
Back | Close
Full Screen / Esc
Printer-friendly Version
Interactive Discussion

as a whole but rather to highlight and correct for a specific problem. The hydrological model used in this study has been well calibrated and validated beforehand. Undoubtedly the performance of rainfall-runoff simulation depends on a wide variety of factors, e.g. the catchment hydrological characteristic, the model rainfall-runoff mechanism, the simulation period and initial conditions; this study only address the contribution of using a better designed depression removal method, whereas in future studies other important aspects such as model bias in whole catchment simulation needs to be taken into account.

Computing wise, this algorithm inherits the advantages of Wang and Liu's (2006) algorithm compared with other traditional depression filling approaches. It directly computes a spill elevation value for each grid cell without prior delineation of the catchments of depressions and progressively builds the optimal flow paths and propagates spill elevation values from outlets to interior grid cells, due to the employment of the least-cost search algorithm. Consequently, it is able to produce the DEM with fewer depressions and identify the locations and depth of the surface depressions with computational time complexity in $O(N \log N)$, which can be easily implemented using object-oriented programming languages like C++ and Java.

Acknowledgements. Thanks are due to Mike Butts and colleagues at the Danish Hydraulics Institute (DHI) for access to MIKE SHE and for their continuous intellectual advice and support throughout.

References

Abbott, M. B., Bathurst, J. C., Cunge, J. A., O'Connell, P. E., and Rasmussen, J.: An introduction to the European Hydrological System – Système Hydrologique Européen "SHE" 1: history and philosophy of a physically-based distributed modelling system, J. Hydrol., 87, 45–59, 1986.

Arnold, J. G., Allen, P. N., and Bernhardt, G.: A comprehensive surface-groundwater flow model, J. Hydrol., 142, 47–69, 1993.

Bates, P. D. and De Roo, A. P. J.: A simple raster-based model for flood inundation simulation, J. Hydrol., 236, 54–57, 2000.
Beven, K. J., Lamb, R., Quinn, P. F., Romanowicz, R., and Freer, J.: TOPMODEL, in: Computer Models of Watershed Hydrology, edited by: Singh, V. P., Water Resources Publications, Highlands Ranch, 627–668, 1995.
Chaplot, V.: Impact of DEM mesh size and soil map scale on SWAT runoff, sediment, and NO_3-N loads predictions, J. Hydrol., 312, 207–222, 2005.
Chaubey, I., Cotter, A. S., Costello, T. A., and Soerens, T. S.: Effect of DEM data resolution on SWAT output uncertainty, Hydrol. Process., 19, 621–628, 2005.
Christiaens, K. and Feyen, J.: Constraining soil hydraulic parameter and output uncertainty of the distributed hydrological MIKE SHE model using the GLUE framework, Hydrol. Process., 16, 373–391, 2002.
DHI: MIKE SHE, An Integrated Hydrological Modelling System: User Guide, DHI Software 2007, 2007.
Fairfield, J. and Leymarie, P.: Drainage networks from grid digital elevation models, Water Resour. Res., 27, 709–717, 1991.
Jain, S. K., Storm, B., Bathurst, J. C., Refsgaard, J. C., and Singh, R. D.: Application of the SHE to catchments in India – Part 2: field experiments and simulation studies on the Kolar Subcatchment of the Narmada River, J. Hydrol., 140, 25–47, 1992.
Lane, S. N.: Hydraulic modelling in hydrology and geomorphology: a review of high resolution approaches, Hydrol. Process., 12, 1131–1150, 1998.
Lea, N. L.: An aspect driven kinematic routing algorithm, in: Overland Flow: Hydraulics and Erosion Mechanics, edited by: Parsons, A. J. and Abrahams, A. D., Chapman Hall, New York, 147–175, 1992.
Madsen, H.: Parameter estimation in distributed hydrological catchment modelling using automatic calibration with multiple objectives, Adv. Water Resour., 26, 205–216, 2003.
Maksimović, Č., Prodanović, D., Boonya-Aroonnet, S., Leitão, J. P., Djordjevic, S., and Allitt, R: Overland flow and pathway analysis for modelling of urban pluvial flooding, J. Hydraul. Res., 47, 512–523, 2009.
Maidment, D. R. (Ed.): Arc Hydro: GIS for Water Resources [EB/OL], ESRI Press, 2002.
Martz, L. W. and Garbrecht, J.: The treatment of flat areas and depressions in automated drainage analysis of raster digital elevation models, Hydrol. Process., 12, 843–845, 1998.

HESSD
9, 10011–10051, 2012

DEM-based 2-dimensional surface flow modelling

D. Zhu et al.

O'Brien, J. S., Julien, P. Y., and Fullerton, W. T.: Two-dimensional water flood and mudflow simulation, J. Hydraul. Eng., 119, 244–261, 1993.
O'Callaghan, J. and Mark, D.: The extraction of drainage networks from digital elevation data, Comput. Vis. Graph Image Process., 28, 323–344, 1984.
Refsgaard, J. C. and Knudsen, J.: Operational validation and intercomparison of different types of hydrological models, Water Resour. Res. 32, 2189–2202, 1996.
Singh, V. P: Computer Models of Watershed Hydrology, Water Resources Publications, Colorado, USA, 1995.
Tarboton, D. G.: A new method for the determination of flow directions and upslope areas in grid digital elevation models, Water Resour. Res., 33, 309–319, 1997.
Vázquez, R. F. and Feyen, J.: Assessment of the effects of DEM gridding on the predictions of basin runoff using MIKE SHE and a modelling resolution of 600 m, J. Hydrol. 334, 73–87, 2007.
Vázquez, R. F., Feyen, L., Feyen, J., and Refsgaard, J. C.: Effect of grid size on effective parameters and model performance on the MIKE SHE code, Hydrol. Process., 16, 355–372, 2002.
Wang, L. and Liu, H.: An efficient method for identifying and filling surface depressions in digital elevation models for hydrologic analysis and modeling, Int. J. Geogr. Inf. Sci., 20, 193–213, 2006.
Wheater, H. S.: Progress in and prospects for fluvial flood modelling, Philos. Trans. Royal Soc. London, 360, 1409–1431, 2002.
Wolock, D. M. and Price, C. V.: Effects of digital elevation model map scale and data resolution on a topography-based watershed model., Water Resour. Res., 30, 3041–3052, 1994.
Xevi, E., Christiaens, K., Espino, A., Sewnandan, W., Mallants, D., Sorensen, H., and Feyen, J.: Calibration, validation and sensitivity analysis of the MIKE SHE model using the Neuenkirchen catchment as case study, Water Resour. Manage., 11, 219–239, 1997.
Yu, D. and Lane, S. N.: Urban fluvial flood modelling using a two-dimensional diffusion-wave treatment, Part 1: mesh resolution effects. Hydrol. Process., 20, 1541–1565, 2006.
Yu, P.-S.: Real-time Grid Based Distributed Rainfall-Runoff Model for Flood Forecasting with Weather Radar, Ph.D. Thesis, University of Birmingham, Birmingham, 1987.
Zhu, D.: A Comparative Study of Single and Dual Polarisation Quantitative Weather Radar in the Context of Hydrological Modelling Structure, Ph.D. Thesis, University of Bristol, Bristol, 2009.

HESSD
9, 10011–10051, 2012
DEM-based 2-dimensional surface flow modelling
D. Zhu et al.

Table 1. Pseudo-code for algorithm implementation.

```
For b ← [cells on data boundary or channel cells]
  Spill[b] ← Elevation[b]
  PQueue.push(b)
  Mark[b]=true
End For

While PQueue is not empty
  c ← PQueue.top()
  PQueue.pop(c)
  Mark[c] ← true
  For n ← [4 neighbors of c]
    If Mark[n]=true
      Then [do nothing]
    Else
      Spill[n] ← Max(Elevation[n],Spill[c])
      PQueue.push(n)
    End If
  End For
End While
```


HESSD
9, 10011–10051, 2012

DEM-based 2-dimensional surface flow modelling

D. Zhu et al.

Table 2. Statistics of slopes (unit: degree) and elevations (unit: m).

DEM Type	Minimum		Maximum		Mean		Standard deviation	
	Slope	Elevation	Slope	Elevation	Slope	Elevation	Slope	Elevation
50 m original	0	20.20	24.14	241.90	4.17	98.66	2.66	39.93
50 m filled	0	20.20	24.14	241.90	4.13	98.69	2.65	39.90
100 m original	0	20.30	16.84	241.96	3.57	98.66	2.12	39.94
100 m filled	0	20.30	16.84	241.96	3.50	98.78	2.10	39.88
200 m original	0	20.69	11.87	241.04	2.74	98.66	1.57	39.92
200 m filled	0	20.69	11.87	241.05	2.66	99.06	1.55	39.78

HESSD
9, 10011–10051, 2012

Table 3. Statistics of the depression using DEM differences (unit: m).

DEM resolution	Minimum	Maximum	Mean	Standard deviation
50 m	0	9.1	0.030	0.227
100 m	0	14.86	0.123	0.713
200 m	0	25.62	0.461	1.814

HESSD
9, 10011–10051, 2012

DEM-based 2-dimensional surface flow modelling

D. Zhu et al.

Table 4. Statistics of the peak flow in whole catchment simulations.

DEM type	Peak flow difference (unit: $m^3 s^{-1}$)	Percentage of peak outflow difference	Percentage of total outflow difference
50 m original	−6.55	−17.17 %	11.21 %
50 m filled	−6.41	−16.81 %	11.57 %
100 m original	−6.79	−17.83 %	10.51 %
100 m filled	−3.54	−9.28 %	13.02 %
200 m original	−4.62	−12.11 %	10.88 %
200 m filled	1.31	3.45 %	13.51 %

HESSD
9, 10011–10051, 2012

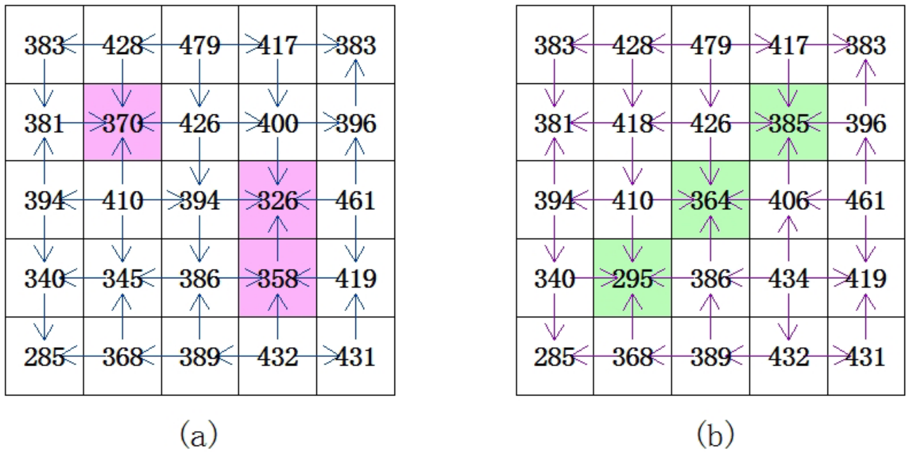

Fig. 1. Example of two types of DEM depression.

HESSD
9, 10011–10051, 2012

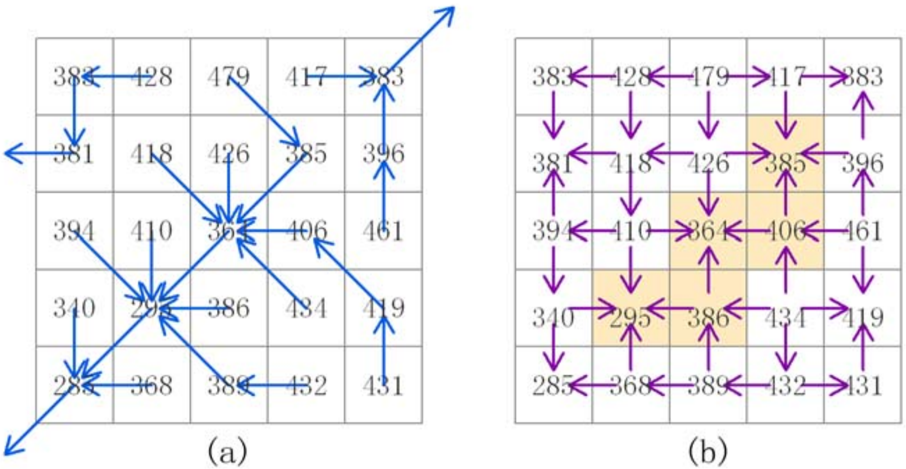

Fig. 2. Overland flow paths processed by D8 and MIKE SHE.

HESSD

9, 10011–10051, 2012

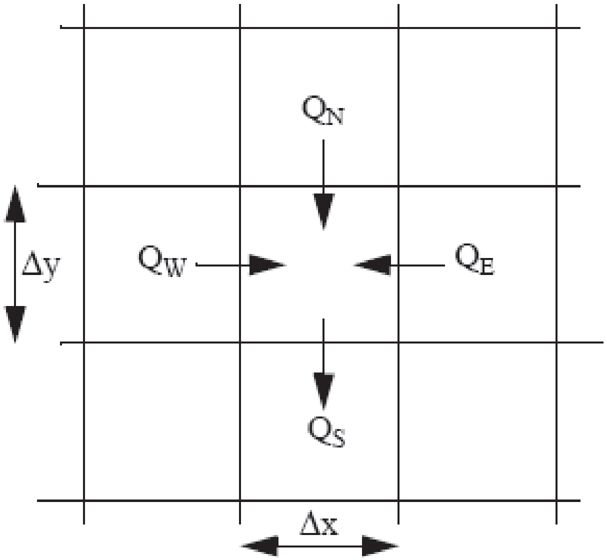

Fig. 3. Demonstration of flow on a square grid system in MIKE SHE model (source: DHI, 2007).

HESSD
9, 10011–10051, 2012

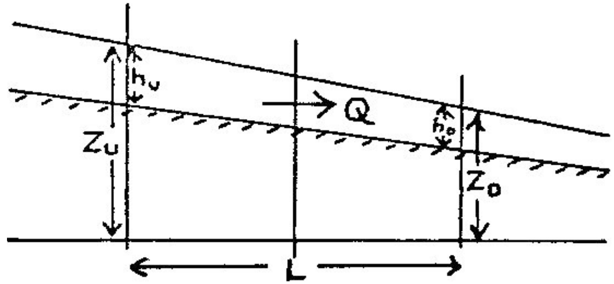

Fig. 4. Demonstration of overland flow across the square grid boundary (source: DHI, 2007).

HESSD
9, 10011–10051, 2012

DEM-based 2-dimensional surface flow modelling

D. Zhu et al.

383	428	479	417	383
381	418	426	396	396
394	410	386	406	461
340	340	386	434	419
285	368	389	432	431

(a)

1	2	3	4	5
6	20	24	25	7
8	19	22	23	9
10	17	18	21	11
12	13	14	15	16

(b)

Fig. 5. DEM with depression removal algorithm applied and the relevant processing order.

HESSD
9, 10011–10051, 2012

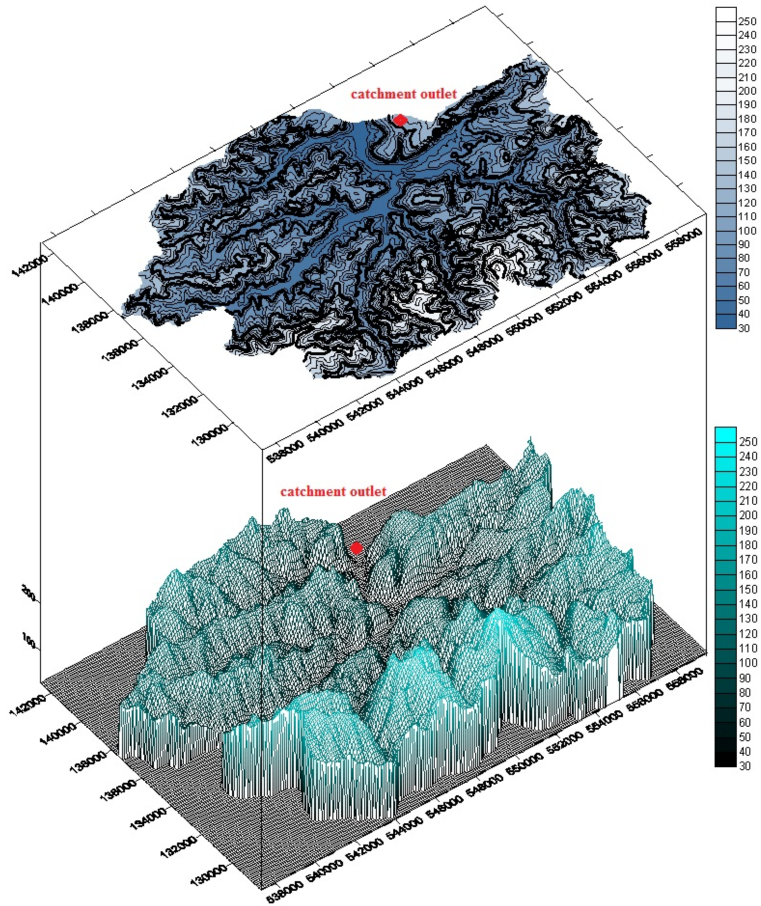

Fig. 6. Contours and DEM for the upper medway catchment (unit: m). The X- and Y-axis stand for the easting and northing coordinates of catchment.

HESSD
9, 10011–10051, 2012

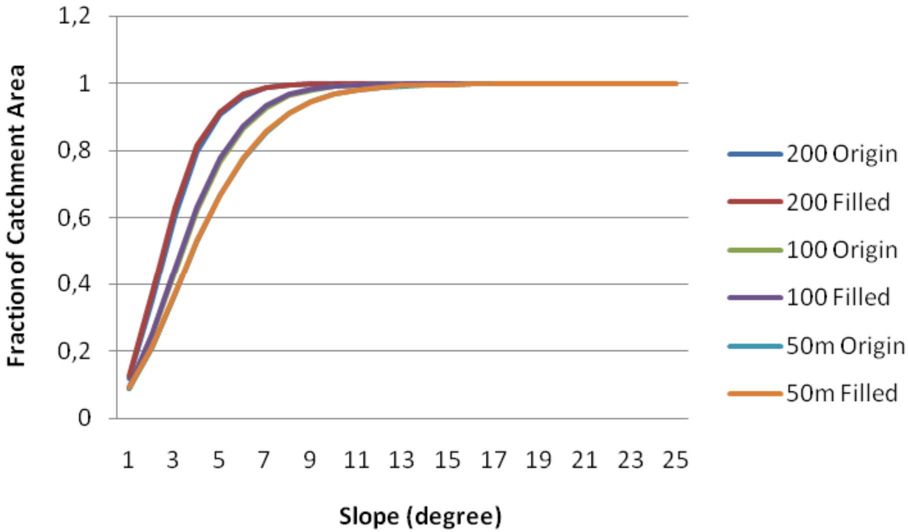

Fig. 7. Cumulative distributions of DEM slopes.

HESSD
9, 10011–10051, 2012

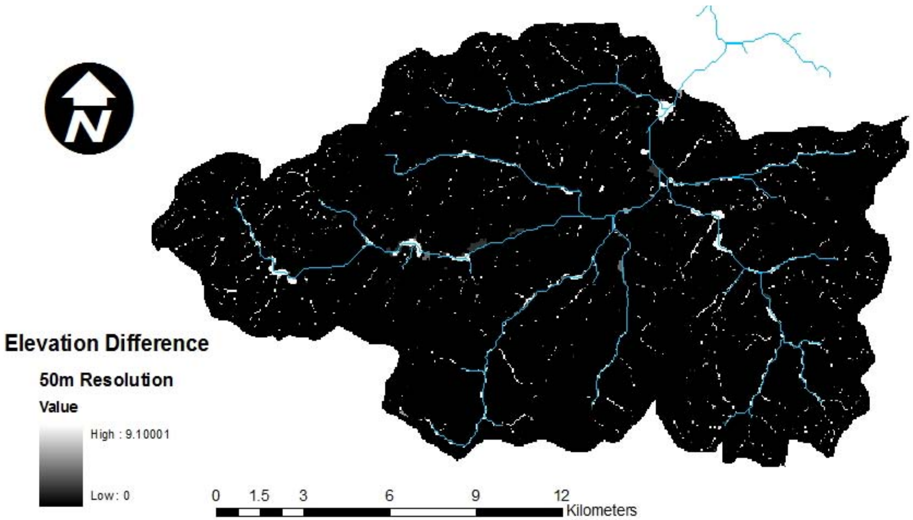

Fig. 8. Elevation differences for the 50 m resolution DEM for upper medway catchment.

HESSD
9, 10011–10051, 2012

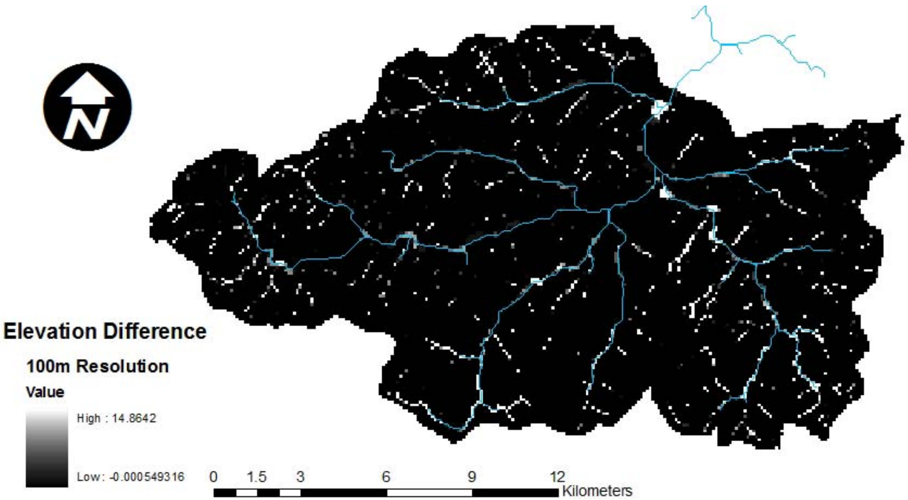

Fig. 9. Elevation differences for the 100 m resolution DEM for upper medway catchment.

HESSD
9, 10011–10051, 2012

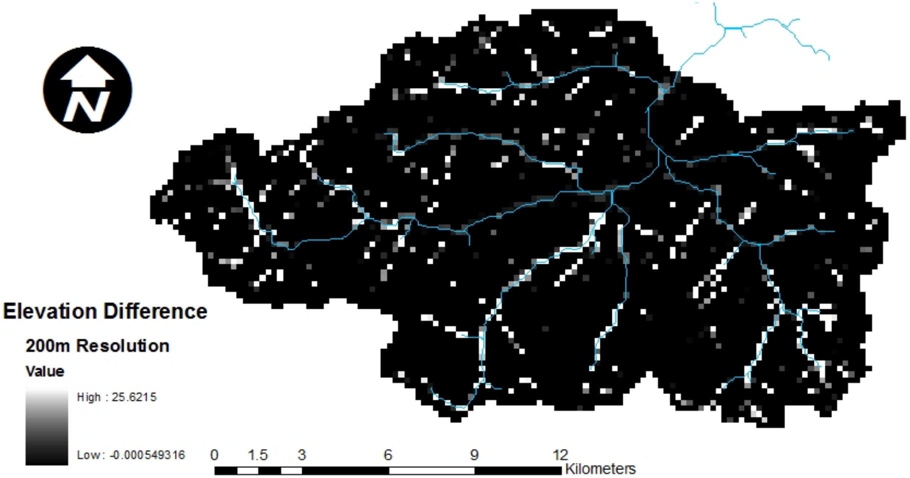

Fig. 10. Elevation differences for the 200 m resolution DEM for upper medway catchment.

HESSD
9, 10011–10051, 2012

DEM-based 2-dimensional surface flow modelling

D. Zhu et al.

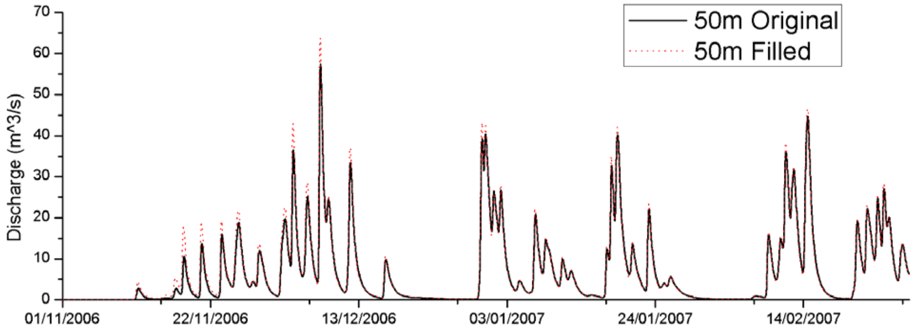

Fig. 11. Surface flow simulations for the 50 m resolution DEM in MIKE SHE.

HESSD
9, 10011–10051, 2012

DEM-based 2-dimensional surface flow modelling

D. Zhu et al.

Title Page
Abstract | Introduction
Conclusions | References
Tables | Figures
◀| |▶
◀ ▶
Back | Close
Full Screen / Esc
Printer-friendly Version
Interactive Discussion

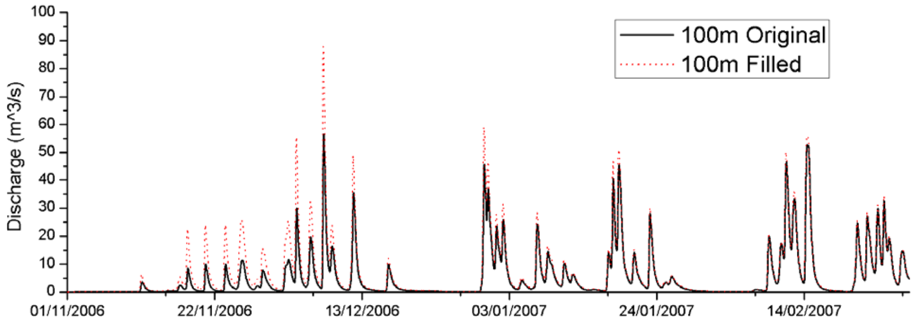

Fig. 12. Surface flow simulations for the 100 m resolution DEM in MIKE SHE.

HESSD
9, 10011–10051, 2012

DEM-based 2-dimensional surface flow modelling

D. Zhu et al.

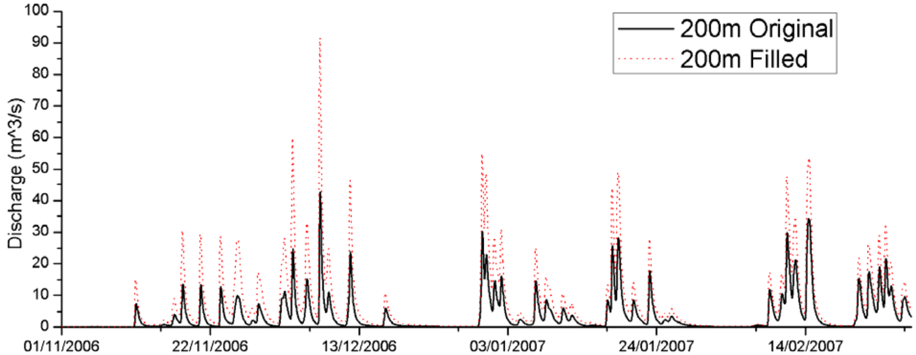

Fig. 13. Surface flow simulations for the 200 m resolution DEM in MIKE SHE.

HESSD
9, 10011–10051, 2012

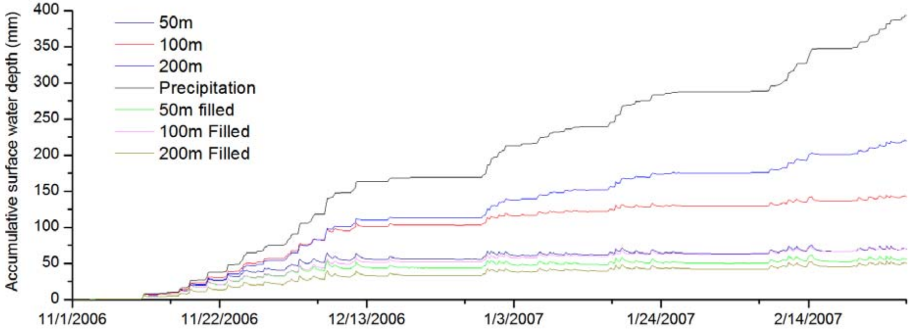

Fig. 14. Accumulative surface water depths during model simulations.

HESSD
9, 10011–10051, 2012

DEM-based 2-dimensional surface flow modelling

D. Zhu et al.

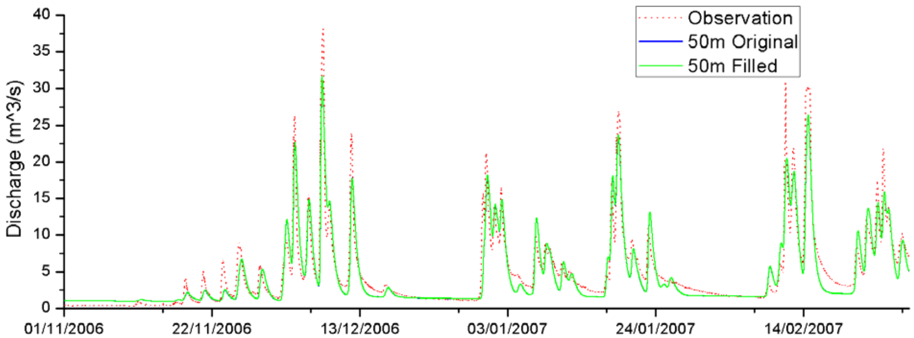

Fig. 15. Whole catchment flow simulations using 50 m resolution DEM in MIKE SHE.

HESSD
9, 10011–10051, 2012

DEM-based 2-dimensional surface flow modelling

D. Zhu et al.

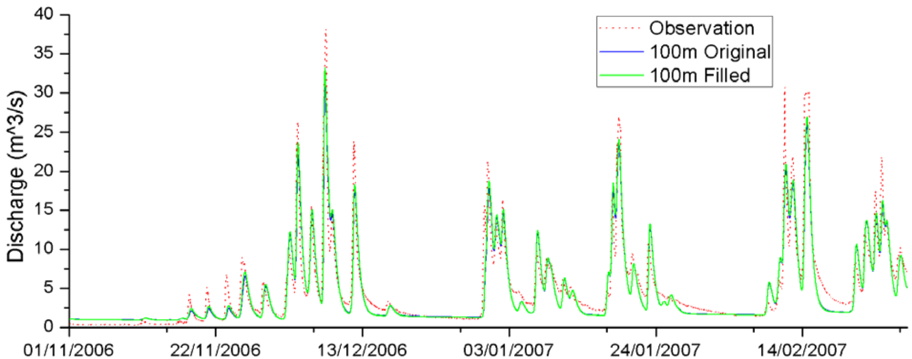

Fig. 16. Whole catchment flow simulations using 100 m resolution DEM in MIKE SHE.

HESSD
9, 10011–10051, 2012

DEM-based 2-dimensional surface flow modelling

D. Zhu et al.

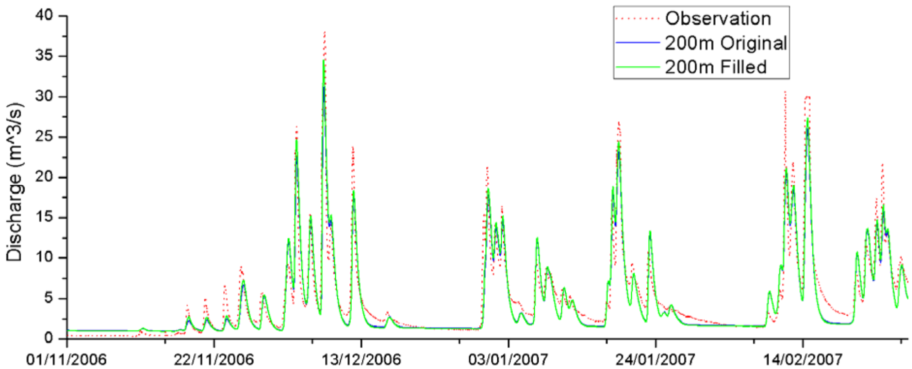

Fig. 17. Whole catchment flow simulations using 200 m resolution DEM in MIKE SHE.

HESSD
9, 10011–10051, 2012

DEM-based 2-dimensional surface flow modelling

D. Zhu et al.